

Exact transcendental stiffness matrices of general beam-columns embedded in elastic mediums

Sondipon Adhikari

Zienkiewicz Centre for Computational Engineering, College of Engineering, Swansea University, Swansea, UK



ARTICLE INFO

Article history:

Received 20 December 2020

Accepted 15 June 2021

Keywords:

Beam-column
Elastic foundation
Bending deformation
Stiffness matrix
Exact solutions
Transcendental shape function

ABSTRACT

Stiffness matrices of beams embedded in an elastic medium and subjected to axial forces are considered. Both the bending and the axial deformations have been incorporated. Two approaches for deriving the element stiffness matrix analytically have been proposed. The first approach is based on the direct force–displacement relationship, whereas the second approach exploits shape functions within the finite element framework. The displacement function within the beam is obtained from the solution of the governing differential equation with suitable boundary conditions. Both approaches result in identical expressions when the exact transcendental displacement functions are used. Exact closed-form expressions of the elements of the stiffness matrix have been derived for the bending and axial deformation. Depending on the nature of the axial force and stiffness of the elastic medium, seven different cases are proposed for the bending stiffness matrix. A unified approach to the non-dimensional representation of the stiffness matrix elements and system parameters that are consistent across all the cases has been developed. Through Taylor-series expansions of the stiffness matrix coefficients, it is shown that the classical stiffness matrices appear as an approximation when only the first few terms of the series are retained. Numerical results shown in the paper explicitly quantify the error in using the classical stiffness compared to the exact stiffness matrix derived in the paper. The expressions derived here gives the most comprehensive and consistent description of the stiffness coefficients, which can be directly used in the context of finite element analysis over a wide range of parameter values.

© 2021 Elsevier Ltd. All rights reserved.

1. Introduction

The analysis of beam and beam-columns on elastic foundation is a traditional topic. The impact of beam theory spans across different length scales. At small length scales, beam theory has been used for nanoscale structures such as carbon nanotubes and microtubules. At the macro scale, beam theories have been used for larger structures such as aircraft wings and long-distance pipelines. The striking fact is that beam theory with suitable adaptations has provided simple mechanical and physical justifications of observed results beyond any other simple mechanics-based theories. For this reason, in spite of being a classical topic, the mechanics of beams is still an important research area and likely to remain so in the near future. Carrera unified formulation [1] is an excellent example of an advanced beam theory. Relatively recent developments in size-dependent structural beam theories, such as nonlocal [2,3], hybrid nonlocal [4] and strain gradient-based approaches [5,6] have further increased the relevance of beam theories on contemporary developments.

Although the analysis of ‘individual’ beams using the theory of continuum mechanics is physically insightful and numerically accurate, extending this approach to complex built-up structures with thousands of beams is not straightforward. In this case, the stiffness matrix of an elemental beam can be assembled to represent the mechanics of the global system. The accuracy and computational efficiency of the approach depend on two crucial factors, namely, (a) the ability of the beam element stiffness matrix to capture the true physics of the deformation patterns within the beam and (b) the number of finite elements used to represent the global mechanical behaviour of the system. The aim of an efficient approach is to have a stiffness matrix which truly captures the deformation mechanics of a beam such that a minimum number of finite elements are used to capture the global response behaviour under prescribed external forces. Several authors have proposed beam element stiffness matrices towards these directions. For a beam without any axial forcing and not resting on an elastic foundation, the internal deflection is exactly expressed by a cubic polynomial. The classical stiffness matrix of a beam is derived [7–10] using cubic polynomial shape functions within the scope of finite element formulation. For the more general case of

E-mail address: S.Adhikari@swansea.ac.uk

beam-columns on elastic foundation, the displacement function is expressed by transcendental functions (see for example [11,12]). Sirosh et al. [13] used exponential form of the displacement function and numerically obtained the stiffness matrix of a general beam-column with tensile axial force. Yankelevsky and Eisenberger [11], on the other hand, considered compressive axial force and obtained the coefficients of the 4×4 stiffness matrix in closed-form using transcendental functions. For the same problem, Razaqpur [14] independently obtained the stiffness matrix numerically and the equivalent nodal force analytically. Karamanlidis and Prakash [15] obtained the element stiffness matrix in closed-form for a beam-column with a two-parameter elastic foundation. While these formulations consider Euler–Bernoulli beam theory, equivalent analysis is also available for more general Timoshenko beams (see for example [16,17]).

From this brief discussion, it is clear that extensive references are available for the exact stiffness matrix of Euler–Bernoulli beams under the most general case. In spite of these excellent results, the vast majority of commercial software and research literature still uses beam element stiffness matrix based on the classical beam finite element stiffness matrix founded on the cubic shape functions [7]. The reason behind this include, but are not limited to: (1) lack of clarity and consistency in defining the element stiffness coefficients, (2) the absence of a universal parameterisation approach, and perhaps most importantly, (3) explicitly quantifying the impact on the accuracy of using classical stiffness matrix in comparison to the exact stiffness matrix. In this paper, all of these three identified aspects are addressed rigorously and comprehensively.

The paper is organised as follows. In Section 2, the conventional stiffness matrices using the classical cubic shape functions have been reviewed. Two different approaches to obtain the exact stiffness matrix have been proposed for the general beam-column on an elastic foundation. In Section 3 the exact stiffness matrix of a beam with an axial force is considered. Expressions are derived for both compressive and tensile forces. The stiffness matrix when the beam is resting on an elastic foundation is derived in Section 4. The most general case is discussed in Section 5 where in addition to the elastic foundation, an axial force is also considered. Based on different parameter combinations, four sub-cases are considered. In Section 6, the exact stiffness matrix for the axial deformation is derived in terms of hyperbolic functions. For all the cases, the stiffness matrix elements have been obtained analytically and expressed by closed-form expressions. Finally, in Section 7 some conclusions are drawn based on the results obtained in the paper.

2. A general derivation of the exact stiffness matrix

We consider a general Euler–Bernoulli beam-column resting on an elastic foundation as shown in Fig. 1. Different parameters which govern the deflection of the beam are shown in the figure. In this section, we first briefly review the conventional finite element approach for the derivation of the general stiffness matrix.

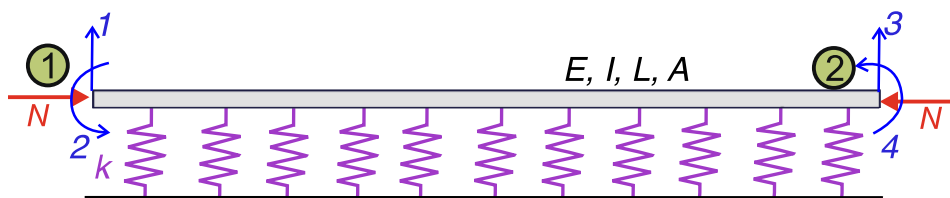


Fig. 1. An Euler–Bernoulli beam on an elastic foundation subjected to an axial force. Here A is the cross-sectional area, E is Young’s modulus of the material, I is second the moment of area, k is the stiffness per unit length of the elastic foundation, N is the axial force, and L is the length of the beam. Different boundary conditions can be applied at both ends of the beam.

Then two distinct approaches are proposed to obtain the general stiffness matrix exactly. The first approach, developed in Section 2.2, is a physics-based approach that exploits the force–displacement relationship of the beam. The second approach developed in Section 2.3 is a theoretical approach that utilises the exact shape function of the beam.

2.1. The conventional finite element approach for a general beam-column

The transverse deflection of the beam shown in Fig. 1 is governed by a fourth-order following ordinary differential equation (see for example [8,9,7]) as

$$EI \frac{d^4 W(x)}{dx^4} + N \frac{d^2 W(x)}{dx^2} + kW(x) = F(x) \tag{1}$$

Here N is the axial force, k is the stiffness per unit length of the elastic foundation, EI is the bending rigidity of the beam, $W(x)$ is transverse displacement. In the above equation, $F(x)$ is externally applied distributed transverse force on the beam (not explicitly shown in Fig. 1). The elastic foundation is assumed to be the ‘Winkler Foundation’. This implies that the interface between the beam and the springs as shown in Fig. 1 satisfies the displacement compatibility condition [18].

The beam element has two nodes and four degrees of freedom. The displacement field within the element is expressed by cubic shape functions [7] for the classical finite element analysis and they are given by

$$\mathbf{N}(\xi) = \left[2\xi^3 - 3\xi^2 + 1, L\xi(\xi - 1)^2, -2\xi^3 + 3\xi^2, L\xi^2(\xi - 1) \right]^T \tag{2}$$

In the above, the non-dimensional length variable is expressed as $\xi = x/L$

Note that these shape functions do not arise from the exact solution of the governing differential Eq. (1) with relevant boundary conditions. Employing these shape functions in conjunction with the conventional variational formulation [7], the stiffness matrix of the general beam element can be obtained as

$$\begin{aligned} \mathbf{K} &= EI \int_0^L \frac{d^2 \mathbf{N}(x)}{dx^2} \frac{d^2 \mathbf{N}^T(x)}{dx^2} dx - N \int_0^L \frac{d\mathbf{N}(x)}{dx} \frac{d\mathbf{N}^T(x)}{dx} dx + k \int_0^L \mathbf{N}(x) \mathbf{N}^T(x) dx \\ &= \frac{EI}{L^3} \int_0^1 \frac{d^2 \mathbf{N}(\xi)}{d\xi^2} \frac{d^2 \mathbf{N}^T(\xi)}{d\xi^2} d\xi - \frac{N}{L} \int_0^1 \frac{d\mathbf{N}(\xi)}{d\xi} \frac{d\mathbf{N}^T(\xi)}{d\xi} d\xi + kL \int_0^1 \mathbf{N}(\xi) \mathbf{N}^T(\xi) d\xi \\ &= \frac{EI}{L^3} \int_0^1 \left(\frac{d^2 \mathbf{N}(\xi)}{d\xi^2} \frac{d^2 \mathbf{N}^T(\xi)}{d\xi^2} - v^2 \frac{d\mathbf{N}(\xi)}{d\xi} \frac{d\mathbf{N}^T(\xi)}{d\xi} + 4\eta^4 \mathbf{N}(\xi) \mathbf{N}^T(\xi) \right) d\xi \end{aligned} \tag{4}$$

In the above equation, the non-dimensional axial force and the non-dimensional foundation stiffness are given by

$$v^2 = \frac{NL^2}{EI} \tag{5}$$

$$\text{and } \eta^4 = \frac{kL^4}{4EI} \tag{6}$$

Evaluating the integral in Eq. (4) and simplifying we have the classical stiffness matrix of the beam-column on an elastic foundation corresponding to Fig. 1 as

$$\mathbf{K} = \frac{EI}{L^3} \begin{bmatrix} d_1 & d_2L & -d_5 & d_6L \\ & d_3L^2 & -d_6L & d_4L^2 \\ \text{sym} & & d_1 & -d_2L \\ & & & d_3L^2 \end{bmatrix} \quad (7)$$

where

$$\begin{aligned} d_1 &= 12 - \frac{6}{5}v^2 + \frac{52\eta^4}{35}, & d_2 &= 6 - \frac{1}{10}v^2 + \frac{22\eta^4}{105}, & d_3 &= 4 - \frac{2}{15}v^2 + \frac{4\eta^4}{105} \\ d_4 &= 2 + \frac{1}{30}v^2 - \frac{\eta^4}{35}, & d_5 &= d_1 & \text{and} & d_6 &= d_2 \end{aligned} \quad (8)$$

In the absence of the axial force and the foundation stiffness, that is when $v = \eta = 0$, the above expression reduces to the conventional stiffness matrix of Euler–Bernoulli beams as

$$\mathbf{K}_{EB} = \mathbf{K}_{(v=\eta=0)} = \frac{EI}{L^3} \begin{bmatrix} 12 & 6L & -12 & 6L \\ 6L & 4L^2 & -6L & 2L^2 \\ -12 & -6L & 12 & -6L^2 \\ 6L & 2L^2 & -6L & 4L^2 \end{bmatrix} \quad (9)$$

Although the integral in Eq. (4) is evaluated exactly in deriving the stiffness matrix, the error in employing this matrix in the context of the finite element analysis arises from the fact that the displacement field within the beam is not exactly represented by the cubic polynomials used in the shape function in Eq. (2). As a result, a larger number of elements need to be used in solving practical problems. Despite these limitations, the stiffness coefficients expressed by Eq. (8) are widely used for their simplicity and convenience. In this paper, we are focusing on closed-form expressions of stiffness matrices of 1D elements. Note that for 2D and 3D elements with complex shapes, it is more common to obtain integrals as Eq. (4) numerically, for example, using a Gaussian quadrature [19] method. In the rest of the paper, the integrals appearing in the derivation of the stiffness matrix are obtained analytically.

2.2. The method based on force–displacement relationships

In contrast to the preceding case, if the stiffness matrix is derived using the exact displacement field, only one ‘element’ will be necessary for an entire beam (as in the special case with (7) when $v = \eta = 0$). Therefore, it is vitally important to obtain the exact stiffness matrix of the beam element. For the general case, transforming Eq. (1) in the non-dimensional coordinate ξ we have

$$\frac{d^4w(\xi)}{d\xi^4} + v^2 \frac{d^2w(\xi)}{d\xi^2} + 4\eta^4w(\xi) = 0 \quad (10)$$

Here $w(\xi) \equiv W(x)$ and the forcing is assumed to be zero. Assuming a solution of the form

$$w(\xi) = \exp[\lambda\xi] \quad (11)$$

and substituting in Eq. (10) results in the characteristics equation

$$\lambda^4 + v^2\lambda^2 + 4\eta^4 = 0 \quad (12)$$

This equation will result in four roots for λ as $\lambda_1 \dots, \lambda_4$. Considering these roots, the general solution can be expressed as

$$w(\xi) = \mathbf{s}^T(\xi)\mathbf{c} \quad (13)$$

Here the vectors of basis functions and unknown constants are given by

$$\mathbf{s}^T(\xi) = \{\exp[\lambda_1\xi], \exp[\lambda_2\xi], \exp[\lambda_3\xi], \exp[\lambda_4\xi]\} \quad (14)$$

$$\text{and } \mathbf{c} = \{c_1, c_2, c_3, c_4\}^T \quad (15)$$

In general the roots of (12) are complex valued. Therefore, it is often convenient to express the basis functions in terms of real valued trigonometric and hyperbolic functions.

The natural boundary conditions of the beam are expressed in terms of the displacement $W(x)$, rotation $(\Theta(x))$, bending moment $(M(x))$ and shear force $(V(x))$. They are given by

$$\Theta(x) = \frac{dW(x)}{dx} \equiv \frac{1}{L} \frac{dw(\xi)}{d\xi} \quad (16)$$

$$M(x) = EI \frac{d^2W(x)}{dx^2} \equiv \frac{EI}{L^2} \frac{d^2w(\xi)}{d\xi^2} \quad (17)$$

$$\begin{aligned} \text{and } -V(x) &= EI \frac{d^3W(x)}{dx^3} + N \frac{dW(x)}{dx} \equiv \frac{EI}{L^3} \left(\frac{d^3w(\xi)}{d\xi^3} + v^2 \frac{dw(\xi)}{d\xi} \right) \\ &= \frac{EI}{L^3} \mathcal{L}[w(\xi)] \end{aligned} \quad (18)$$

where the operator

$$\mathcal{L} \equiv \frac{d^3}{d\xi^3} + v^2 \frac{d}{d\xi} \quad (19)$$

The nodal displacement vector of the beam consists of the displacement and rotation of the beam at the two ends. This can be obtained in terms of the displacement function $w(\xi)$ in Eq. (13) as

$$\delta = \begin{Bmatrix} W_1 \\ \Theta_1 \\ W_2 \\ \Theta_2 \end{Bmatrix} = \begin{Bmatrix} W(0) \\ \Theta(0) \\ W(L) \\ \Theta(L) \end{Bmatrix} = \begin{Bmatrix} w(0) \\ \frac{1}{L}w'(0) \\ w(1) \\ \frac{1}{L}w'(1) \end{Bmatrix} = \underbrace{\begin{bmatrix} \mathbf{s}^T(0) \\ \frac{1}{L}\mathbf{s}'^T(0) \\ \mathbf{s}^T(1) \\ \frac{1}{L}\mathbf{s}'^T(1) \end{bmatrix}}_{\mathcal{A}_{4 \times 4}} \mathbf{c} \quad (20)$$

In the above equation $(\bullet)'$ denotes the derivative with respect to ξ . The nodal force vector consists of the shear force and bending moment at the two ends of the beam. The displacement function $w(\xi)$ in Eq. (13) can be used to obtain them as

$$\mathbf{f} = \begin{Bmatrix} V_1 \\ M_1 \\ V_2 \\ M_2 \end{Bmatrix} = \begin{Bmatrix} -V(0) \\ -M(0) \\ V(L) \\ M(L) \end{Bmatrix} = \frac{EI}{L^3} \underbrace{\begin{bmatrix} \mathcal{L}[\mathbf{s}^T(0)] \\ -L\mathbf{s}''^T(0) \\ -\mathcal{L}[\mathbf{s}^T(1)] \\ L\mathbf{s}''^T(1) \end{bmatrix}}_{\mathcal{B}_{4 \times 4}} \mathbf{c} \quad (21)$$

In the above equation $(\bullet)''$ denotes the second derivative with respect to ξ . Eliminating the constant vector \mathbf{c} from the previous two equations we obtain a direct relationship between the nodal force and displacement vectors as

$$\mathbf{f} = \underbrace{\frac{EI}{L^3} [\mathcal{B}\mathcal{A}^{-1}]}_{\mathcal{K}_{4 \times 4}} \delta \quad (22)$$

Here \mathcal{K} is the exact stiffness matrix, which can be obtained in closed-form using the expression derived above. The derivation proposed here does not use the shape functions and consequently avoids the determination of integrals similar to what encountered in Eq. (4).

2.3. The method based on the exact shape functions

The force–displacement approach proposed in the previous section is simple and exact. However, it is valid only when the exact solution of the displacement function is available. Another issue with the above method is that if there are distributed body forces within the beam, there are no simple ways to take it into account within the context of a finite element formulation. The shape function-based approach to be proposed here addresses these drawbacks.

Table 1
The relationship between the boundary conditions and the shape functions.

	$N_1(\xi)$	$N_2(\xi)$	$N_3(\xi)$	$N_4(\xi)$
$W(0) = w(0)$	1	0	0	0
$\Theta(0) = \frac{1}{L}w'(0)$	0	1	0	0
$W(L) = w(1)$	0	0	1	0
$\Theta(L) = \frac{1}{L}w'(1)$	0	0	0	1

Using the displacement function in Eq. (13), the vector of shape functions are expressed as

$$\mathbf{N}(\xi) = \begin{Bmatrix} N_1(\xi) \\ N_2(\xi) \\ N_3(\xi) \\ N_4(\xi) \end{Bmatrix} = \begin{bmatrix} \mathbf{c}_1^T \\ \mathbf{c}_2^T \\ \mathbf{c}_3^T \\ \mathbf{c}_4^T \end{bmatrix} \mathbf{s}(\xi) \quad (23)$$

Here \mathbf{c}_j is the vector of constants giving rise to the j th shape function. These unknown constants need to be obtained from the boundary conditions which define the shape functions. The relationship between the shape functions and the boundary conditions can be represented as in Table 1, where boundary conditions in each column give rise to the corresponding shape function. Writing Eq. (13) for the above four sets of boundary conditions, one obtains

$$\mathcal{A}[\mathbf{c}_1, \mathbf{c}_2, \mathbf{c}_3, \mathbf{c}_4] = \mathbf{I} \quad (24)$$

In the above \mathbf{I} is a 4×4 identity matrix and the matrix \mathcal{A} was defined in Eq. (20). Solving the above equation for the unknown constants and substituting in Eq. (23) we obtain the exact shape functions as

$$\mathbf{N}(\xi) = [\mathcal{A}^{-1}]^T \mathbf{s}(\xi) \quad (25)$$

Substituting this in the integral expression of the stiffness matrix in Eq. (4), we obtain

$$\mathcal{K} = \frac{EI}{L^3} \mathcal{A}^{-1T} \left\{ \int_0^1 \left(\frac{d^2 \mathbf{s}(\xi)}{d\xi^2} \frac{d^2 \mathbf{s}^T(\xi)}{d\xi^2} - v^2 \frac{d\mathbf{s}(\xi)}{d\xi} \frac{d\mathbf{s}^T(\xi)}{d\xi} + 4\eta^2 \mathbf{s}(\xi) \mathbf{s}^T(\xi) \right) d\xi \right\} \mathcal{A}^{-1} \quad (26)$$

This is an alternate expression to the one derived in the previous section. The matrix \mathcal{K}_e is termed here as the *elementary stiffness matrix* and it depends only on the basis functions and not on the boundary conditions. When exact shape functions are used, both equations give identical results. The expression of the shape function in Eq. (26) can be used to obtain nodal forces arising due to the distributed body forces. Considering $f(\xi) \equiv F(x)$ we obtain

$$\mathbf{p} = \int_0^1 \mathbf{N}(\xi) f(\xi) d\xi = \mathcal{A}^{-1T} \int_0^1 \mathbf{s}(\xi) f(\xi) d\xi \mathbf{p}_e \quad (27)$$

The vector \mathbf{p}_e is called the *elementary body force* vector. In view of the stiffness matrix and the forcing vector, the equilibrium equation of the beam is given by

$$\mathcal{K} \mathbf{w} = \mathbf{p} \quad (28)$$

where \mathbf{w} is the nodal response vector. Substituting the expressions of the stiffness matrix and the forcing vector from Eqs. (26) and (27) we have

$$\left(\frac{EI}{L^3} \mathcal{A}^{-1T} \mathcal{K}_e \mathcal{A}^{-1} \right) \mathbf{w} = \mathcal{A}^{-1T} \mathbf{p}_e \quad \text{or} \quad \mathbf{w} = \frac{L^3}{EI} \mathcal{A} \mathcal{K}_e^{-1} \mathbf{p}_e \quad (29)$$

Using the nodal response vector, the displacement field within the beam can be obtained using the shape functions as

$$w(\xi) = \mathbf{N}^T(\xi) \mathbf{w} = \mathbf{s}^T(\xi) \mathcal{A}^{-1} \frac{L^3}{EI} \mathcal{A} \mathcal{K}_e^{-1} \mathbf{p}_e = \frac{L^3}{EI} \mathbf{s}^T(\xi) (\mathcal{K}_e^{-1} \mathbf{p}_e) \quad (30)$$

It is interesting to note that the displacement field is independent of the \mathcal{A} matrix. Next, we apply the general theory proposed in this section to some physically realistic special cases.

3. Beam-columns with axial forces

A beam-column with an axial force N is shown in Fig. 2. The transverse deflection of the beam is governed by a fourth-order ordinary differential equation given in (1) with $k = 0$. The characteristics equation is given by

$$\lambda^4 + v^2 \lambda^2 = 0 \quad \text{or} \quad \lambda^2 (1 + v^2) = 0 \quad (31)$$

The four solutions of the above equation are

$$\lambda^2 = 0, \lambda = \pm iv \quad \text{or} \quad \lambda_{1,2,3,4} = 0, 0, \pm iv \quad (32)$$

Using these solutions, the vector of basis functions is obtained as

$$\mathbf{s}^T(\xi) = \{e^{(0, \pm iv)\xi}\} = \{1, \xi, \sin v\xi, \cos v\xi\} \quad (33)$$

From Eqs. (20) and (21), the matrices \mathcal{A} and \mathcal{B} are derived using the above basis functions as

$$\mathcal{A} = \begin{bmatrix} 1 & 0 & 0 & 1 \\ 0 & L^{-1} & \frac{v}{L} & 0 \\ 1 & 1 & \sin(v) & \cos(v) \\ 0 & L^{-1} & \frac{v \cos(v)}{L} & -\frac{v \sin(v)}{L} \end{bmatrix} \quad \text{and} \quad (34)$$

$$\mathcal{B} = \begin{bmatrix} 0 & v^2 & 0 & 0 \\ 0 & 0 & 0 & Lv^2 \\ 0 & -v^2 & 0 & 0 \\ 0 & 0 & -Lv^2 \sin(v) & -Lv^2 \cos(v) \end{bmatrix}$$

Employing these matrices, from Eq. (22) the exact stiffness matrix is obtained in closed-form similar to the classical case in (7) as

$$\mathcal{K} = \frac{EI}{L^3} \mathcal{B} \mathcal{A}^{-1} = \frac{EI}{L^3} \begin{bmatrix} d_1 & d_2L & -d_5 & d_6L \\ & d_3L^2 & -d_6L & d_4L^2 \\ \text{sym} & & d_1 & -d_2L \\ & & & d_3L^2 \end{bmatrix} \quad (35)$$

where

$$d_1 = -\frac{v^3 \sin(v)}{\Delta}, \quad d_2 = \frac{v^2(\cos(v) - 1)}{\Delta}$$

$$d_3 = \frac{v(v \cos(v) - \sin(v))}{\Delta}, \quad d_4 = \frac{v(\sin(v) - v)}{\Delta} \quad (36)$$

$$d_5 = d_1 \quad d_6 = d_2 \quad \text{and} \quad \Delta = v \sin(v) - 2(1 - \cos(v))$$

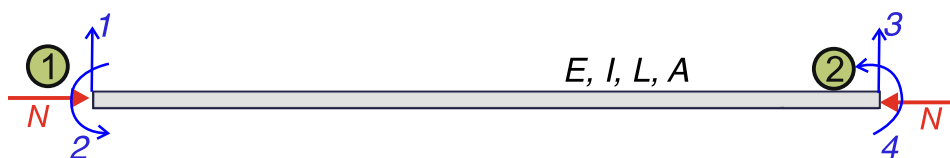


Fig. 2. An Euler-Bernoulli beam subjected to an axial force N .

In the above expressions, the axial force is considered to be compressive in nature. If the axial force is tensile, the sign of v^2 will be negative. Following a similar procedure, it can be shown that the coefficients are expressed in terms of hyperbolic functions. The four unique coefficients are given by

$$\begin{aligned} \bar{d}_1 &= \frac{v^3 \sinh(v)}{\Delta}, \quad \bar{d}_2 = \frac{v^2(\cosh(v) - 1)}{\Delta} \\ \bar{d}_3 &= \frac{v(v \cosh(v) - \sinh(v))}{\Delta}, \quad \bar{d}_4 = \frac{v(\sinh(v) - v)}{\Delta} \quad \text{and} \\ \Delta &= v \sinh(v) - 2 \cosh(v) + 2 \end{aligned} \tag{37}$$

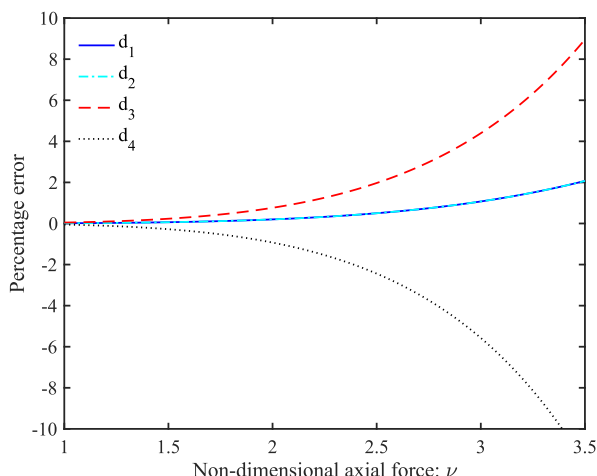
Here the notation \bar{d} is used to distinguish it from the case of compressive force in (36).

The stiffness matrix derived in Eq. (35) uses the method based on the force–displacement relationships developed in Section 2.2. The exact shape function based method described in Section 2.3 can also be used to obtain the same result. After some algebraic simplification, the vector of shape-functions can be derived as

$$\begin{Bmatrix} N_1(\xi) \\ N_2(\xi) \\ N_3(\xi) \\ N_4(\xi) \end{Bmatrix} = \begin{bmatrix} \frac{v \cos(v) - \sin(v) + v}{v \cos(v) - 2 \sin(v) + v} & -\frac{v \sin(v)}{v \sin(v) + 2 \cos(v) - 2} & \frac{\sin(v)}{v \sin(v) + 2 \cos(v) - 2} & -\frac{\sin(v)}{v \cos(v) - 2 \sin(v) + v} \\ \frac{L(v \cos(v) - \sin(v))}{v(v \sin(v) + 2 \cos(v) - 2)} & \frac{L \sin(v)}{v \cos(v) - 2 \sin(v) + v} & \frac{L(-\sin(v) + v(\cos(v) + 1))}{v(-2 \sin(v) + v(\cos(v) + 1))} & \frac{L(v \cos(v) - \sin(v))}{v(v \sin(v) + 2 \cos(v) - 2)} \\ \frac{\sin(v)}{v \cos(v) - 2 \sin(v) + v} & \frac{v \sin(v)}{v \sin(v) + 2 \cos(v) - 2} & -\frac{\sin(v)}{v \sin(v) + 2 \cos(v) - 2} & \frac{\sin(v)}{v \cos(v) - 2 \sin(v) + v} \\ \frac{L(v - \sin(v))}{v(v \sin(v) + 2 \cos(v) - 2)} & \frac{L \sin(v)}{v \cos(v) - 2 \sin(v) + v} & \frac{L \sin(v)}{v(v \cos(v) - 2 \sin(v) + v)} & \frac{L(\sin(v) - v)}{v(v \sin(v) + 2 \cos(v) - 2)} \end{bmatrix} \begin{Bmatrix} 1 \\ \xi \\ \sin(v\xi) \\ \cos(v\xi) \end{Bmatrix} \tag{38}$$

There are four unique non-dimensional coefficients in the stiffness matrix. They are functions of the axial force parameter v only. Expanding them in a Taylor series about $v = 0$ we obtain

$$\begin{aligned} d_1 &= 12 - \frac{6}{5}v^2 - \frac{1}{700}v^4 - \frac{1}{63000}v^6 - \frac{37}{194040000}v^8 - \frac{59}{25225200000}v^{10} + O(v^{12}) \\ d_2 &= 6 - \frac{1}{10}v^2 - \frac{1}{1400}v^4 - \frac{1}{126000}v^6 - \frac{37}{388080000}v^8 - \frac{59}{50450400000}v^{10} + O(v^{12}) \\ d_3 &= 4 - \frac{2}{15}v^2 - \frac{11}{6300}v^4 - \frac{1}{27000}v^6 - \frac{582120000}{509}v^8 - \frac{681080400000}{14617}v^{10} + O(v^{12}) \\ d_4 &= 2 + \frac{1}{30}v^2 + \frac{13}{12600}v^4 + \frac{11}{378000}v^6 + \frac{1164240000}{136216080000}v^8 + \frac{27641}{136216080000}v^{10} + O(v^{12}) \end{aligned} \tag{39}$$



(a) The axial force is compressive

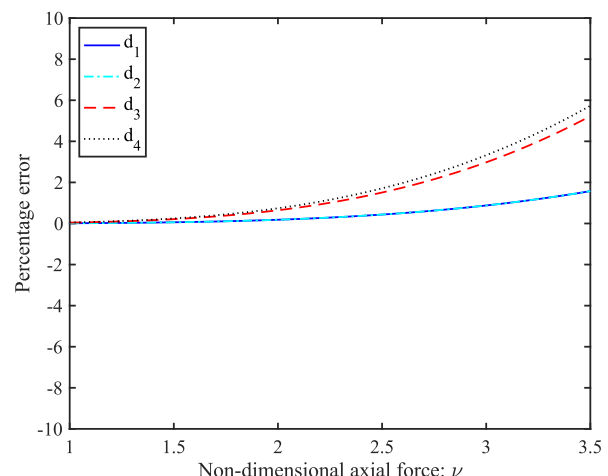
Considering only the first two terms in the above expansion, it can be confirmed that the stiffness matrix derived here reduces to the classical case in Eq. (7). The higher-order terms, therefore, quantify the extended effect of the axial force on the transverse deflection of the beam. This analysis explicitly connects the transcendental stiffness coefficients with the classical stiffness coefficients.

The case considered here as in Fig. 2 is vitally important for the finite element analysis of beams and frames when buckling is investigated. The coefficient matrix associated with the factor v^2 is known as the tangent stiffness matrix. A generalised eigenvalue problem involving the usual stiffness matrix and the tangent stiffness matrix can be solved to obtain different critical buckling loads and their corresponding buckling modes. The stiffness matrix coefficients derived in Eq. (36) incorporate the tangent stiffness matrix in an implicit manner. One needs to solve a non-linear eigenvalue problem arising from the determinant of the global generalised stiffness matrix to obtain the critical buckling loads. As the critical buckling loads are real and positive valued quantities, an algorithm such as the Wittrick-Williams algorithm [20] can be used to effi-

ciently obtain them [21]. Wittrick-Williams algorithm has been successfully applied to extract undamped natural frequencies. Further research is needed for its application in buckling analysis using the stiffness coefficients in Eq. (36).

To understand the error introduced from the use of the classical finite element stiffness matrix, we introduce a new error measure. For a given stiffness coefficient, $d_k, k = 1, \dots, 6$, the error norm is defined as

$$\varepsilon_k = 100 \times \frac{d_{k\text{classical}} - d_k}{d_{k\text{EB}}}, \quad k = 1, 2, \dots, 6 \tag{40}$$



(b) The axial force is tensile

Fig. 3. Errors in the four unique stiffness coefficients obtained using the classical approach in comparison with the exact transcendental stiffness coefficients as functions of the non-dimensional axial force v .

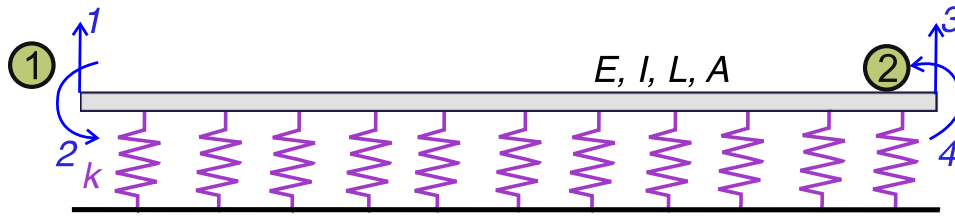


Fig. 4. A Euler-Bernoulli beam on elastic foundation with stiffness per unit length k .

In the above equation, d_{kEB} are the stiffness coefficients from the conventional Euler–Bernoulli beam given in Eq. (9). The multiplication with 100 in the above equation ensures that the error is obtained as a percentage. In Fig. 3, this error is shown for the four unique coefficients for different values of the non-dimensional axial force ν . Both cases, namely when the axial force is compressive and when the axial force is tensile, are shown. Note the difference in the behaviour of the errors for the two case. The error is more when the force is compressive. We observe that for higher values of the compressive axial force, the error can go up to 10%. If many elements are used (such as a complex framed structure), then the difference between using the exact transcendental stiffness matrix and the classical stiffness matrix can be significant. In addition to the accuracy, the use of the transcendental stiffness matrix will contribute to the computational efficiency as only one element is necessary for a physical beam (that is, no internal discretisation is necessary). Geometric non-linearity (also known as the ‘P- δ ’ effect) is included in the formulation of the stiffness matrix coefficients in (36). However, material nonlinearity and large deformation are not considered. Therefore, the stiffness matrix derived should be used for problems involving small deformation.

4. Beams on elastic foundation

In Fig. 2 we show a beam resting on an elastic foundation with stiffness per unit length k . The transverse deflection of the beam is governed by a fourth-order following ordinary differential equation given in (1) with $N = 0$. The characteristics equation is given by

$$\lambda^4 + 4\eta^4 = 0 \tag{41}$$

Using these solutions, the vector of basis functions is obtained as

$$\begin{aligned} \mathbf{s}^T(\xi) &= \{e^{(\pm 1 \pm i)\eta\xi}\} \\ &= \{\sin \eta\xi \sinh \eta\xi, \sin \eta\xi \cosh \eta\xi, \cos \eta\xi \sinh \eta\xi, \cos \eta\xi \cosh \eta\xi\} \end{aligned} \tag{43}$$

From Eqs. (20) and (21), the matrices \mathcal{A} and \mathcal{B} can be derived in closed-form. Using these matrices, from Eq. (22) the stiffness matrix is obtained in closed-form in exactly the same form as in Eq. (35) with the six unique coefficients given by

$$\begin{aligned} d_1 &= 2 \frac{\eta^2(\sinh(\eta) \cosh(\eta) + \sin(\eta) \cos(\eta))}{\Delta}, \\ d_2 &= - \frac{\eta((\cos(\eta))^2 - (\cosh(\eta))^2)}{\Delta}, \\ d_3 &= - \frac{\sin(\eta) \cos(\eta) - \sinh(\eta) \cosh(\eta)}{\Delta}, \\ d_4 &= \frac{\sin(\eta) \cosh(\eta) - \sinh(\eta) \cos(\eta)}{\Delta}, \\ d_5 &= 2 \frac{\eta^2(\sin(\eta) \cosh(\eta) + \sinh(\eta) \cos(\eta))}{\Delta}, \\ d_6 &= 2 \frac{\sin(\eta)\eta \sinh(\eta)}{\Delta} \end{aligned} \tag{44}$$

and $\Delta = \frac{\sinh^2 \eta - \sin^2 \eta}{2\eta}$

The stiffness matrix coefficients derived in Eq. (44) uses the method based on the force–displacement relationships developed in Section 2.2. The exact shape function based method described in Section 2.3 can also be used to obtain the same result. After some algebraic simplification, the vector of shape-functions can be derived as

$$\begin{Bmatrix} N_1(\xi) \\ N_2(\xi) \\ N_3(\xi) \\ N_4(\xi) \end{Bmatrix} = \begin{bmatrix} \frac{(\cos(\xi))^2 - (\cosh(\xi))^2}{(\cos(\xi))^2 + (\cosh(\xi))^2 - 2} & \frac{\sinh(\xi) \cosh(\xi) + \sin(\xi) \cos(\xi)}{(\cos(\xi))^2 + (\cosh(\xi))^2 - 2} & \frac{-\sinh(\xi) \cosh(\xi) - \sin(\xi) \cos(\xi)}{(\cos(\xi))^2 + (\cosh(\xi))^2 - 2} & 1 \\ \frac{L(\sin(\xi) \cos(\xi) - \sinh(\xi) \cosh(\xi))}{\xi((\cos(\xi))^2 + (\cosh(\xi))^2 - 2)} & \frac{L(\sinh(\xi))^2}{\xi((\cos(\xi))^2 + (\cosh(\xi))^2 - 2)} & \frac{-L(\sin(\xi))^2}{\xi((\cos(\xi))^2 + (\cosh(\xi))^2 - 2)} & 0 \\ 2 \frac{\sin(\xi) \sinh(\xi)}{(\cos(\xi))^2 + (\cosh(\xi))^2 - 2} & \frac{-\sin(\xi) \cosh(\xi) - \sinh(\xi) \cos(\xi)}{(\cos(\xi))^2 + (\cosh(\xi))^2 - 2} & \frac{\sin(\xi) \cosh(\xi) + \sinh(\xi) \cos(\xi)}{(\cos(\xi))^2 + (\cosh(\xi))^2 - 2} & 0 \\ \frac{L(\sinh(\xi) \cos(\xi) - \sin(\xi) \cosh(\xi))}{\xi((\cos(\xi))^2 + (\cosh(\xi))^2 - 2)} & \frac{L \sin(\xi) \sinh(\xi)}{\xi((\cos(\xi))^2 + (\cosh(\xi))^2 - 2)} & \frac{-L \sin(\xi) \sinh(\xi)}{\xi((\cos(\xi))^2 + (\cosh(\xi))^2 - 2)} & 0 \end{bmatrix} \begin{Bmatrix} \sin \eta\xi \sinh \eta\xi \\ \sin \eta\xi \cosh \eta\xi \\ \cos \eta\xi \sinh \eta\xi \\ \cos \eta\xi \cosh \eta\xi \end{Bmatrix} \tag{45}$$

Solving the above equation, the four solutions for λ can be concisely expressed as

$$\lambda_{1,2,3,4} = (\sqrt[4]{-1})\sqrt{2}\eta = \left(\pm \frac{1}{\sqrt{2}} \pm \frac{i}{\sqrt{2}}\right)\sqrt{2}\eta = (\pm 1 \pm i)\eta \tag{42}$$

There are six unique non-dimensional coefficients in the stiffness matrix. They are functions of the foundation stiffness parameter η only. Expanding them in a Taylor series about $\eta = 0$ we obtain

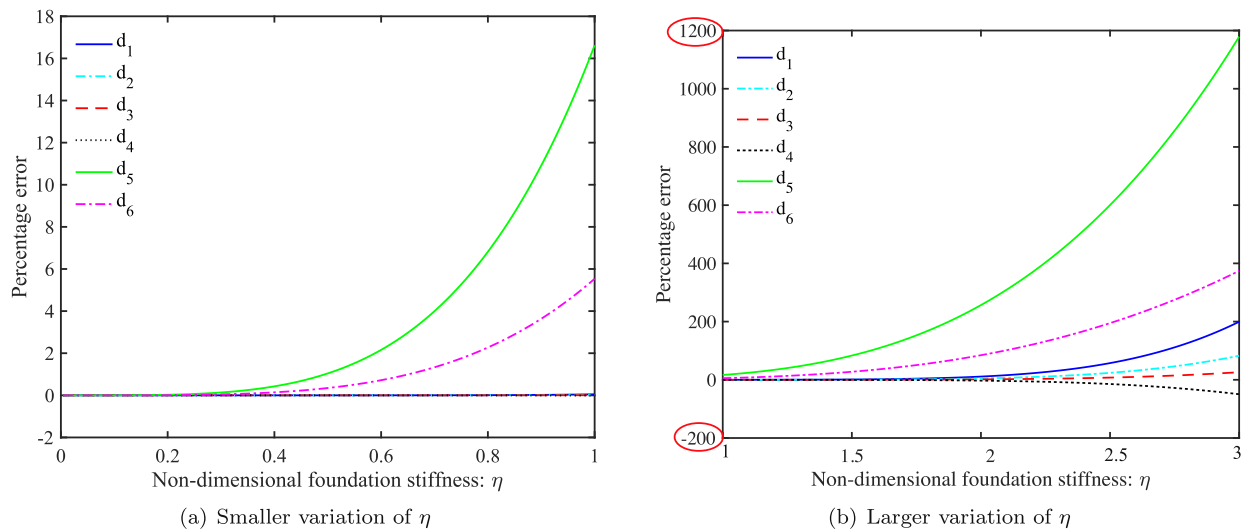


Fig. 5. Errors in the six unique stiffness coefficients obtained using the classical approach in comparison with the exact transcendental stiffness coefficients as functions of the non-dimensional foundation stiffness η .

$$\begin{aligned}
 d_1 &= 12 + \frac{52}{35}\eta^4 - \frac{236}{40425}\eta^8 + \frac{4408}{99324225}\eta^{12} - \frac{3014756}{8551013538375}\eta^{16} + O(\eta^{20}) \\
 d_2 &= 6 + \frac{22}{105}\eta^4 - \frac{446}{363825}\eta^8 + \frac{14188}{1489863375}\eta^{12} - \frac{8430298}{111163175998875}\eta^{16} + O(\eta^{20}) \\
 d_3 &= 4 + \frac{4}{105}\eta^4 - \frac{284}{1091475}\eta^8 + \frac{1016}{496621125}\eta^{12} - \frac{81614284}{5002342919949375}\eta^{16} + O(\eta^{20}) \\
 d_4 &= 2 - \frac{1}{35}\eta^4 + \frac{1097}{4365900}\eta^8 - \frac{899}{441441000}\eta^{12} + \frac{5220181117}{320149946876760000}\eta^{16} + O(\eta^{20}) \\
 d_5 &= 12 - \frac{18}{35}\eta^4 + \frac{1279}{242550}\eta^8 - \frac{5801}{132432300}\eta^{12} + \frac{417329273}{1185740543988000}\eta^{16} + O(\eta^{20}) \\
 d_6 &= 6 - \frac{13}{105}\eta^4 + \frac{1681}{1455300}\eta^8 - \frac{112631}{11918907000}\eta^{12} + \frac{41460911}{547264866456000}\eta^{16} + O(\eta^{20})
 \end{aligned}
 \tag{46}$$

Considering only the first two terms in the above expansion, it can be confirmed that the stiffness matrix derived here reduces to the classical case in Eq. (7) for $d_1 \dots d_4$. The higher-order terms, therefore, quantify the extended effect of the foundation stiffness on the transverse deflection of the beam. This analysis explicitly connects the transcendental stiffness coefficients with the classical stiffness coefficients. (See Fig. 4)

In Fig. 5, the error defined in Eq. (40) is shown for the six unique coefficients for different values of the non-dimensional foundation stiffness η . Two different regimes have been selected, namely, $0 \leq \eta \leq 1$ and $1 \leq \eta \leq 3$. Note the significant difference in the values of the error for the two cases shown in Fig. 5(a) and (b). For values of $\eta > 1$, the difference between using the exact transcendental stiffness matrix and the classical stiffness matrix is significant. For this case, the proposed transcendental stiffness matrix should be used.

5. Beam-columns on an elastic foundation with axial forces

This is the general case considered in Fig. 1. The characteristic equation is given by (12). Its roots are obtained as

$$\lambda^2 = \frac{-v^2 \pm \sqrt{v^4 - 16\eta^4}}{2}
 \tag{47}$$

Depending on the sign of $(v^4 - 16\eta^4)$ and whether the axial force is tensile or compressive, the following four cases arise.

5.1. Case 1: Compressive axial force and $(v^4 - 16\eta^4) \geq 0$

For this case, the solutions given in Eq. (47) can be expressed as

$$\lambda^2 \equiv - \underbrace{\left(\frac{v^2 + \sqrt{v^4 - 16\eta^4}}{2} \right)}_{\alpha^2}, \quad - \underbrace{\left(\frac{v^2 - \sqrt{v^4 - 16\eta^4}}{2} \right)}_{\beta^2}
 \tag{48}$$

It can be easily verified that both α^2 and β^2 are positive and real quantities when $(v^4 - 16\eta^4) \geq 0$. Therefore, the four solutions are given by

$$\begin{aligned}
 \lambda_{1,2,3,4} &= \pm i\alpha, \pm i\beta, \quad \text{where } \alpha \\
 &= \sqrt{\frac{v^2 + \sqrt{v^4 - 16\eta^4}}{2}}, \quad \text{and } \beta \\
 &= \sqrt{\frac{v^2 - \sqrt{v^4 - 16\eta^4}}{2}}, \quad \alpha \geq \beta > 0
 \end{aligned}
 \tag{49}$$

Using these solutions, the vector of basis functions is obtained as

$$\mathbf{s}^T(\xi) = \{e^{\pm i\alpha\xi}, \pm i\beta\xi\} = \{\sin(\alpha\xi), \cos(\alpha\xi), \sin(\beta\xi), \cos(\beta\xi)\}
 \tag{50}$$

It can be deduced that the square-sum of the roots

$$\alpha^2 + \beta^2 = v^2
 \tag{51}$$

Using this, the shear force operator in Eq. (19) can be conveniently expressed in terms of the roots in Eq. (48) as

$$\mathcal{L} \equiv \frac{d^3}{d\xi^3} + (\alpha^2 + \beta^2) \frac{d}{d\xi}
 \tag{52}$$

From Eqs. (20) and (21), the matrices \mathcal{A} and \mathcal{B} are derived using the basis functions in Eq. (50) as

$$\mathcal{A} = \begin{bmatrix} 0 & 1 & 0 & 1 \\ \frac{\alpha}{L} & 0 & \frac{\beta}{L} & 0 \\ \sin(\alpha) & \cos(\alpha) & \sin(\beta) & \cos(\beta) \\ \frac{\alpha \cos(\alpha)}{L} & -\frac{\alpha \sin(\alpha)}{L} & \frac{\beta \cos(\beta)}{L} & -\frac{\beta \sin(\beta)}{L} \end{bmatrix}$$

$$\text{and } \mathcal{B} = \begin{bmatrix} \alpha\beta^2 & 0 & \alpha^2\beta & 0 \\ 0 & L\alpha^2 & 0 & L\beta^2 \\ -\alpha\cos(\alpha)\beta^2 & \alpha\sin(\alpha)\beta^2 & -\beta\cos(\beta)\alpha^2 & \beta\sin(\beta)\alpha^2 \\ -L\alpha^2\sin(\alpha) & -L\alpha^2\cos(\alpha) & -L\beta^2\sin(\beta) & -L\beta^2\cos(\beta) \end{bmatrix} \quad (54)$$

Using these matrices, from Eq. (22) the exact stiffness matrix is obtained in closed-form in exactly the same form as in Eq. (35) with the six unique coefficients give by

$$\begin{aligned} d_1 &= \frac{\alpha\beta(\cos(\alpha)\sin(\beta)\beta - \sin(\alpha)\cos(\beta)\alpha)(-\alpha + \beta)(\alpha + \beta)}{\Delta} \\ d_2 &= -\frac{(\cos(\beta)(\alpha^2 + \beta^2)\cos(\alpha) + 2\sin(\alpha)\sin(\beta)\alpha\beta - \beta^2 - \alpha^2)\beta\alpha}{\Delta} \\ d_3 &= -\frac{(\alpha\cos(\alpha)\sin(\beta) - \sin(\alpha)\beta\cos(\beta))(\alpha^2 - \beta^2)}{\Delta}, \\ d_4 &= \frac{(\sin(\alpha)\beta - \alpha\sin(\beta))(-\alpha^2 + \beta^2)}{\Delta} \\ d_5 &= \frac{\alpha\beta(\alpha\sin(\alpha) - \beta\sin(\beta))(\alpha^2 - \beta^2)}{\Delta}, \\ d_6 &= -\frac{\alpha\beta(\cos(\alpha) - \cos(\beta))(\alpha^2 - \beta^2)}{\Delta} \\ \text{and } \Delta &= -\sin(\beta)(\alpha^2 + \beta^2)\sin(\alpha) - 2\alpha\beta(\cos(\alpha)\cos(\beta) - 1) \end{aligned} \quad (55)$$

These expressions are valid when

$$v^4 - 16\eta^4 \geq 0 \quad \text{or} \quad v \geq 2\eta \quad (56)$$

Next, we consider the case when this condition is not met.

5.2. Case 2: compressive axial force and $(v^4 - 16\eta^4) < 0$

In this case, the square of roots of the characteristics equation given by Eq. (47) will be complex valued as $(v^4 - 16\eta^4)$ is negative. We rewrite them as

$$\lambda^2 = \frac{-v^2 \pm i\sqrt{16\eta^4 - v^4}}{2} \quad (57)$$

It is known that when a and b are positive real numbers, then the square root of the complex number can be expressed by

$$\sqrt{a \pm ib} = \pm \left(\sqrt{\frac{a + \sqrt{a^2 + b^2}}{2}} \pm i\sqrt{\frac{-a + \sqrt{a^2 + b^2}}{2}} \right) \quad (58)$$

Applying this to Eq. (57), all the four roots can be explicitly obtained as

$$\begin{aligned} \lambda_{1,2,3,4} &= \pm\alpha \pm i\beta, \quad \text{where } \alpha = \frac{1}{2}\sqrt{4\eta^2 - v^2}, \beta \\ &= \frac{1}{2}\sqrt{4\eta^2 + v^2}, \quad \beta > \alpha > 0 \end{aligned} \quad (59)$$

Using these solutions, the vector of basis functions is obtained as

$$\begin{aligned} \mathbf{s}^T(\xi) &= \{e^{\pm(\alpha \pm i\beta)\xi}\} \\ &= \{\sinh(\alpha\xi)\sin(\beta\xi), \sinh(\alpha\xi)\cos(\beta\xi), \cosh(\alpha\xi)\sin(\beta\xi), \cosh(\alpha\xi)\cos(\beta\xi)\} \end{aligned} \quad (60)$$

It can be deduced that the square-sum of the roots

$$\beta^2 - \alpha^2 = \frac{1}{2}v^2 \quad (61)$$

Due to this relationship, the shear force operator in Eq. (19) can be conveniently expressed in terms of the roots in Eq. (59) as

$$\mathcal{L} \equiv \frac{d^3}{d\xi^3} + 2(\beta^2 - \alpha^2) \frac{d}{d\xi} \quad (62)$$

From Eqs. (20) and (21), the matrices \mathcal{A} and \mathcal{B} can be derived in closed-form. Using these matrices, from Eq. (22) the exact stiffness matrix is obtained in closed-form in exactly the same form as in Eq. (35) with the six unique coefficients given by

$$\begin{aligned} d_1 &= 2 \frac{\alpha\beta(\alpha^2 + \beta^2)(\cosh(\alpha)\sinh(\alpha)\beta + \sin(\beta)\cos(\beta)\alpha)}{\Delta} \\ d_2 &= \frac{(\alpha^2 + \beta^2)((\cosh(\alpha))^2\beta^2 - (\cos(\beta))^2\alpha^2 + \alpha^2 - \beta^2)}{\Delta} \\ d_3 &= 2 \frac{\alpha\beta(\cosh(\alpha)\sinh(\alpha)\beta - \sin(\beta)\cos(\beta)\alpha)}{\Delta}, \\ d_4 &= 2 \frac{\alpha\beta(\alpha\cosh(\alpha)\sin(\beta) - \sinh(\alpha)\beta\cos(\beta))}{\Delta} \\ d_5 &= 2 \frac{(\alpha\cosh(\alpha)\sin(\beta) + \sinh(\alpha)\beta\cos(\beta))\alpha\beta(\alpha^2 + \beta^2)}{\Delta}, \\ d_6 &= 2 \frac{\alpha\beta\sinh(\alpha)\sin(\beta)(\alpha^2 + \beta^2)}{\Delta} \\ \text{and } \Delta &= (\sinh(\alpha))^2\beta^2 - (\sin(\beta))^2\alpha^2 \end{aligned} \quad (63)$$

The stiffness matrix coefficients in Eq. (63) along with the coefficients in Eq. (55) derived in the previous subsection define the stiffness matrix for the general case of compressive axial force and elastic foundation as shown in Fig. 1 for the complete parametric space of v and η . In Fig. 6, the error defined in Eq. (40) is shown for the six unique coefficients for different values of the non-dimensional foundation stiffness η and non-dimensional axial force v . The plots show contours of percentage errors. The contour marks are labelled clearly in the plots (note the different colour codes in different subplots). All the six coefficients show unique patterns of their errors. For example, coefficients d_1 and d_6 show significant growth in error with increasing η compared to the other four coefficients. There are two generic features in these plots. The first is the top left corner, which is the 'v-dominated' region of error. Here the value of η is small, and hence the stiffness coefficients are obtained from Eq. (63). The straight line in the figure corresponds to the parameter combination $v = 2\eta$. The second key feature is the ' η -dominated' region of error in the right-hand side of the plots. Here, irrespective of the value v , the error becomes large for larger values of η . This observation is consistent with what seen before in Fig. 5 when the variation of only η was considered. The results shown in Fig. 6 provide a strong justification for the use of the exact stiffness coefficient derived here.

5.3. Case 3: Tensile axial force and $(v^4 - 16\eta^4) \geq 0$

When the axial force is tensile, the characteristic equation is given by

$$\lambda^4 - v^2\lambda^2 + 4\eta^4 = 0 \quad (64)$$

The solutions given in Eq. (47) can expressed as

$$\lambda^2 \equiv \underbrace{\frac{v^2 + \sqrt{v^4 - 16\eta^4}}{2}}_{\alpha^2}, \quad \underbrace{\frac{v^2 - \sqrt{v^4 - 16\eta^4}}{2}}_{\beta^2} \quad (65)$$

It can be easily verified that both α^2 and β^2 are positive and real quantities when $(v^4 - 16\eta^4) \geq 0$. Therefore, the four solutions are given by

$$\begin{aligned} \lambda_{1,2,3,4} &= \pm\alpha, \pm\beta, \quad \text{where} \\ \alpha &= \sqrt{\frac{v^2 + \sqrt{v^4 - 16\eta^4}}{2}}, \quad \text{and} \\ \beta &= \sqrt{\frac{v^2 - \sqrt{v^4 - 16\eta^4}}{2}}, \quad \alpha \geq \beta > 0 \end{aligned} \quad (66)$$

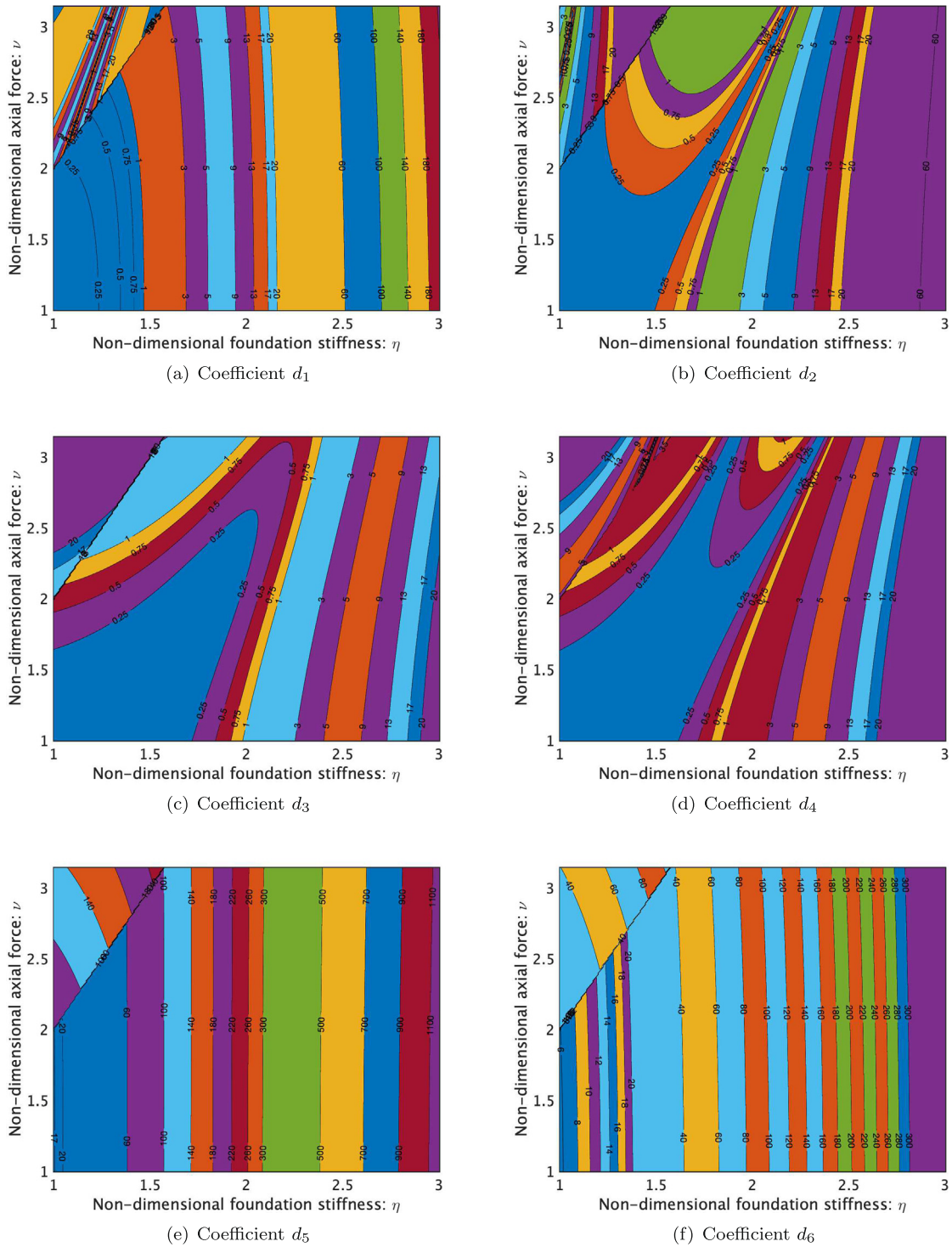


Fig. 6. Contours of percentage errors in the six unique stiffness coefficients obtained using the classical approach in comparison with the exact transcendental stiffness coefficients as functions of the non-dimensional foundation stiffness η and non-dimensional compressive axial force ν .

Using these solutions, the vector of basis functions is obtained as $\mathbf{s}^T(\xi) = \{e^{\pm\alpha\pm\beta\xi}\} = \{\sinh(\alpha\xi), \cosh(\alpha\xi), \sinh(\beta\xi), \cosh(\beta\xi)\}$ (67)

It can be deduced that the square-sum of the roots $\alpha^2 + \beta^2 = \nu^2$ (68)

Due to this relationship, the shear force operator can be expressed in terms of the roots in Eq. (66) as

$$\mathcal{L} \equiv \frac{d^3}{d\xi^3} - (\alpha^2 + \beta^2) \frac{d}{d\xi} \tag{69}$$

From Eqs. (20) and (21), the matrices \mathcal{A} and \mathcal{B} can be derived analytically. Using these matrices, from Eq. (22) the exact stiffness

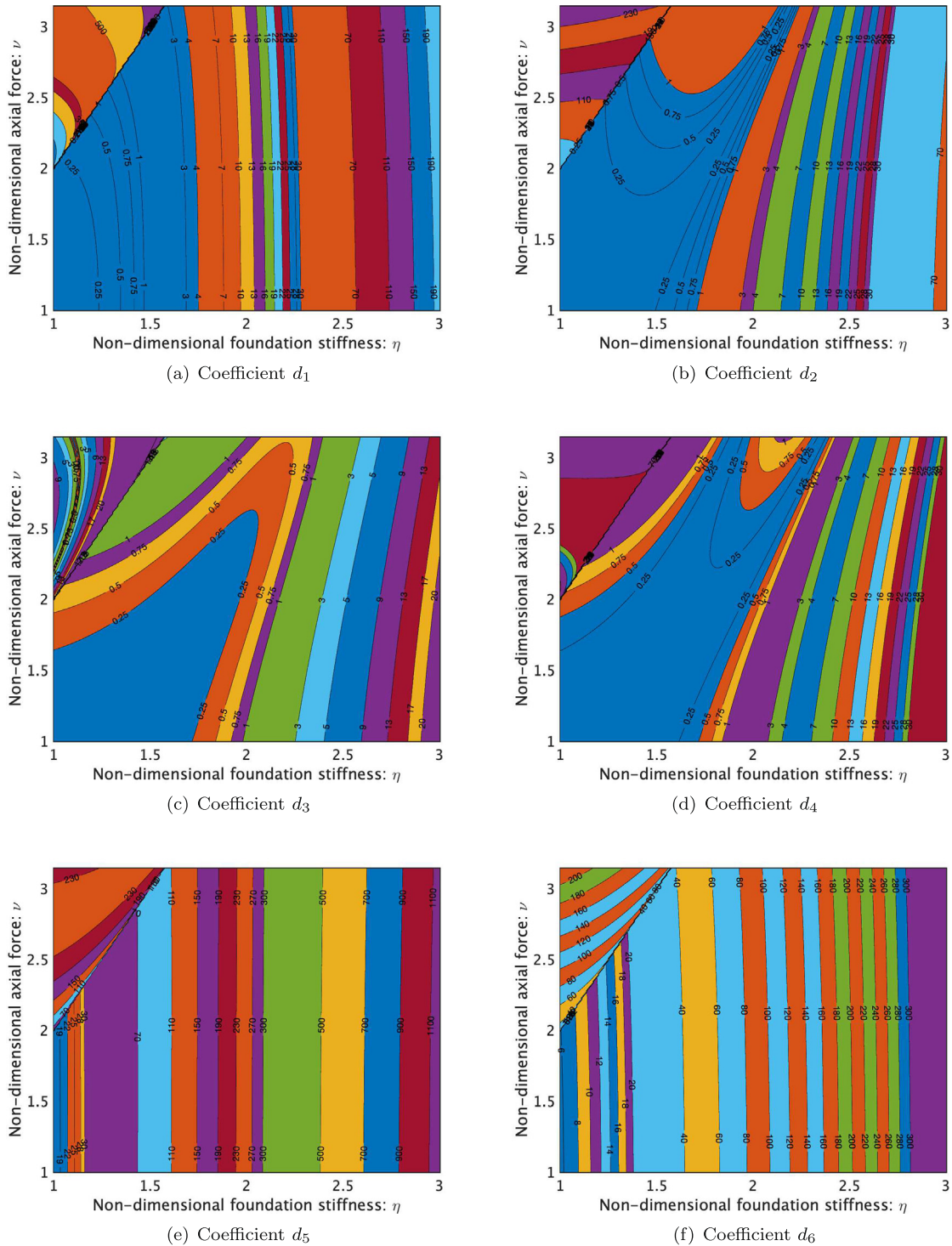


Fig. 7. Contours of percentage errors in the six unique stiffness coefficients obtained using the classical approach in comparison with the exact transcendental stiffness coefficients as functions of the non-dimensional foundation stiffness η and non-dimensional tensile axial force ν .

matrix is obtained in closed-form in exactly the same form as in Eq. (35) with the six unique coefficients given by

$$d_1 = \frac{\alpha\beta(\sinh(\beta)\cosh(\alpha)\beta - \cosh(\beta)\sinh(\alpha)\alpha)(\beta - \alpha)(\beta + \alpha)}{\Delta}$$

$$d_2 = \frac{\alpha(\cosh(\beta)(\alpha^2 + \beta^2)\cosh(\alpha) - 2\sinh(\beta)\sinh(\alpha)\alpha\beta - \beta^2 - \alpha^2)\beta}{\Delta}$$

$$d_3 = \frac{(\alpha\cosh(\alpha)\sinh(\beta) - \sinh(\alpha)\beta\cosh(\beta))(\alpha^2 - \beta^2)}{\Delta}$$

$$d_4 = -\frac{(\beta\sinh(\beta) - \sinh(\alpha)\beta)(\alpha^2 - \beta^2)}{\Delta}$$

$$d_5 = \frac{\alpha\beta(\sinh(\beta)\beta - \sinh(\alpha)\alpha)(-\alpha^2 + \beta^2)}{\Delta}$$

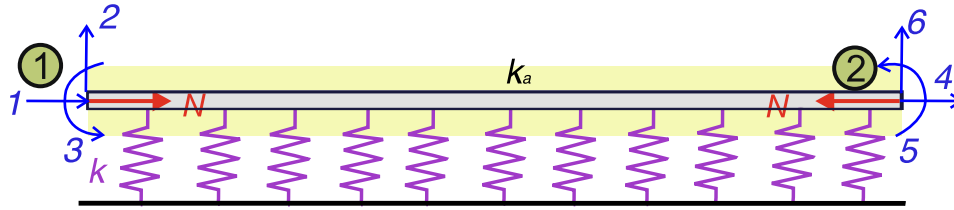


Fig. 8. An Euler–Bernoulli beam embedded in an elastic medium. Here k is the stiffness per unit length of the elastic medium for bending deformation, and k_a is the stiffness per unit length of the elastic medium for axial deformation (marked by the shaded region). The beam element has six degrees of freedom where 1 and 4 correspond to axial deformation, while 2, 3, 5 and 6 correspond to transverse deformation and rotation at the two ends.

$$d_6 = \frac{\alpha \beta (\cosh(\beta) - \cosh(\alpha)) (-\alpha^2 + \beta^2)}{\Delta}$$

and $\Delta = \sinh(\beta) (\alpha^2 + \beta^2) \sinh(\alpha) - 2 \alpha \beta (\cosh(\alpha) \cosh(\beta) - 1)$ (70)

These expressions are valid when $v \geq 2\eta$. Next, we consider the case when this condition is not met.

5.4. Case 4: Tensile axial force and $(v^4 - 16\eta^4) < 0$

In this case, the square of roots of the characteristics equation given by Eq. (56) will be complex valued as $(v^4 - 16\eta^4)$ is negative. We rewrite the solutions in Eq. (65) as

$$\lambda^2 = \frac{v^2 \pm i\sqrt{16\eta^4 - v^4}}{2}$$
 (71)

Using the expression of the square root of a complex number given in (58), all the four roots can be explicitly obtained as

$$\lambda_{1,2,3,4} = \pm\beta \pm i\alpha, \quad \text{where } \alpha = \frac{1}{2}\sqrt{4\eta^2 - v^2}, \beta = \frac{1}{2}\sqrt{4\eta^2 + v^2}, \beta > \alpha > 0$$
 (72)

Note that the real and imaginary parts are swapped in comparison to the case of compressive force given in (59). Using these solutions, the vector of basis functions is obtained as

$$\mathbf{s}^T(\xi) = \{ \sinh(\beta\xi) \sin(\alpha\xi), \sinh(\beta\xi) \cos(\alpha\xi), \cosh(\beta\xi) \sin(\alpha\xi), \cosh(\beta\xi) \cos(\alpha\xi) \}$$
 (73)

It can be deduced that the square-sum of the roots

$$\alpha^2 + \beta^2 = \frac{1}{2}v^2$$
 (74)

The shear force operator can be expressed in terms of the roots in Eq. (72) as

$$\mathcal{L} \equiv \frac{d^3}{d\xi^3} - 2(\beta^2 - \alpha^2) \frac{d}{d\xi}$$
 (75)

From Eqs. (20) and (21), the matrices \mathcal{A} and \mathcal{B} can be derived in closed-form. Using these matrices, from Eq. (22) the exact stiffness matrix is obtained in closed-form in the same form as in Eq. (35) with the six unique coefficients given by

$$d_1 = 2 \frac{\alpha \beta (\alpha^2 + \beta^2) (\cos(\beta) \sin(\beta) \alpha + \sinh(\alpha) \cosh(\alpha) \beta)}{\Delta}$$

$$d_2 = \frac{(\alpha^2 + \beta^2) (-(\cos(\beta))^2 \alpha^2 + (\cosh(\alpha))^2 \beta^2 + \alpha^2 - \beta^2)}{\Delta}$$

$$d_3 = -2 \frac{\alpha \beta (\cos(\beta) \sin(\beta) \alpha - \sinh(\alpha) \cosh(\alpha) \beta)}{\Delta}$$

$$d_4 = -2 \frac{\alpha \beta (\sinh(\alpha) \beta \cos(\beta) - \alpha \cosh(\alpha) \sin(\beta))}{\Delta}$$

$$d_5 = 2 \frac{(\alpha \cosh(\alpha) \sin(\beta) + \sinh(\alpha) \beta \cos(\beta)) \alpha \beta (\alpha^2 + \beta^2)}{\Delta}$$

$$d_6 = 2 \frac{\alpha \beta \sin(\beta) \sinh(\alpha) (\alpha^2 + \beta^2)}{\Delta}$$

and $\Delta = (\sinh(\beta))^2 \alpha^2 - (\sin(\alpha))^2 \beta^2$ (76)

The stiffness matrix coefficients in Eq. (76) along with the coefficients in Eq. (70) derived in the previous subsection define the stiffness matrix for the general case of tensile axial force and elastic foundation as shown in Fig. 1 for the complete parametric space of v and η . In Fig. 7, the error defined in Eq. (40) is shown for the six unique coefficients for different values of the non-dimensional foundation stiffness η and non-dimensional axial force v . Characteristics of these plots are similar to the case of compressive axial force discussed before.

The results obtained in this section are for the most general case. Therefore, the analytical expressions of the stiffness matrix coefficients in Sections 3 and 4 can be obtained as special cases of what is derived here. The case of beam-columns with axial forces only discussed in Section 3 can be recovered by taking $\lim_{\eta \rightarrow 0}$ with cases 2 and 4 depending upon whether the axial force is compressive or tensile. Similarly, the case of beams on elastic foundation in Section 4 can be recovered by taking $\lim_{v \rightarrow 0}$ with cases 1 or 3 (will give the same result).

6. General beam-columns embedded in elastic mediums with axial deformation

6.1. The axial stiffness matrix

So far, only the bending deformation has been considered. However, when the axial deformation, in addition to the bending deformation, is taken into account, we consider k_a as the stiffness per unit length of the elastic medium. In this case, the beam element will have six degrees of freedom as shown in Fig. 8. The axial deformation is uncoupled from the bending deformation for Euler–Bernoulli beams. Therefore the 2×2 stiffness matrix corresponding to the axial deformation can be obtained independently to the bending case considered before. The axial deflection of the beam shown in Fig. 8 is governed by a second-order ordinary differential equation (see for example [9,7]) as

$$EA \frac{d^2 U(x)}{dx^2} - k_a U(x) = F_a(x)$$
 (77)

Here k_a is the stiffness per unit length of the elastic medium, EA is the axial rigidity of the beam, $U(x)$ is axial displacement, and $F_a(x)$ is the applied distributed axial force on the beam. The applied distributed force will contribute towards the element forcing vector, which is not considered in this study. The beam element for the axial case will have two nodes and two degrees of freedom. The axial displacement field within the element is expressed by linear shape functions [7] for the classical finite element analysis, and they are given by

$$\mathbf{N}(\xi) = [1 - \xi, \xi]^T$$
 (78)

where the non-dimensional length variable $\xi = x/L$.

These shape functions do not arise from the exact solution of the governing differential Eq. (77) with relevant boundary conditions. Employing these shape functions in conjunction with the

conventional variational formulation [7], the stiffness matrix of the general beam element can be obtained as

$$\begin{aligned} \mathbf{K}_a &= EA \int_0^L \frac{d\mathbf{N}(x)}{dx} \frac{d\mathbf{N}^T(x)}{dx} dx + k_a \int_0^L \mathbf{N}(x)\mathbf{N}^T(x) dx \\ &= \frac{EA}{L} \int_0^1 \frac{d\mathbf{N}(\xi)}{d\xi} \frac{d\mathbf{N}^T(\xi)}{d\xi} d\xi + k_a L \int_0^1 \mathbf{N}(\xi)\mathbf{N}^T(\xi) d\xi \\ &= \frac{EA}{L} \int_0^1 \left(\frac{d\mathbf{N}(\xi)}{d\xi} \frac{d\mathbf{N}^T(\xi)}{d\xi} + \mu^2 \mathbf{N}(\xi)\mathbf{N}^T(\xi) \right) d\xi \end{aligned} \quad (79)$$

In the above equation, the non-dimensional elastic medium stiffness is given by

$$\mu^2 = \frac{k_a L^2}{EA} \quad (80)$$

Evaluating the integral in Eq. (79) and simplifying we have the classical axial stiffness matrix a the rod embedded in an elastic medium corresponding to Fig. 8 as

$$\mathbf{K}_a = \frac{EA}{L} \begin{bmatrix} a_1 & -a_2 \\ -a_2 & a_1 \end{bmatrix} \quad (81)$$

where

$$a_1 = 1 + \frac{1}{3}\mu^2, \quad \text{and} \quad a_2 = 1 - \frac{1}{6}\mu^2 \quad (82)$$

In the absence of the elastic medium, that is, when $\mu = 0$, the above expression reduces to the conventional stiffness matrix of a rod. The linear shape functions in Eq. (78) do not arise from the exact solution of the governing equation in (77). Consequently, the stiffness matrix coefficients in Eq. (82) are not exact.

Transforming the governing differential Eq. (77) in the non-dimensional coordinate we have

$$\frac{d^2 u(\xi)}{d\xi^2} - \mu^2 u(\xi) = 0 \quad (83)$$

Here $u(\xi) \equiv U(x)$ and the forcing is assumed to be zero. Assuming a solution of the form $u(\xi) = \exp[\lambda\xi]$ and substituting in Eq. (83) results in the characteristics equation

$$\lambda^2 - \mu^2 = 0 \quad (84)$$

This equation will result in two roots for λ and consequently the general solution can be expressed as

$$u(\xi) = \mathbf{s}^T(\xi)\mathbf{c} \quad (85)$$

Here the vectors of basis functions and unknown constants are given by

$$\mathbf{s}^T(\xi) = \{\sinh(\mu\xi), \cosh(\mu\xi)\} \quad \text{and} \quad \mathbf{c} = \{c_1, c_2\}^T \quad (86)$$

The natural boundary conditions are expressed in terms of the displacement $U(x)$ and the axial force $H(x)$

$$-H(x) = EA \frac{dU(x)}{dx} = \frac{EA}{L} \frac{du(\xi)}{d\xi} \quad (87)$$

The nodal displacement vector consists of the displacements at the two ends. This can be obtained in terms of the displacement function $u(\xi)$ in Eq. (85) as

$$\delta = \begin{Bmatrix} U_1 \\ U_2 \end{Bmatrix} = \begin{Bmatrix} U(0) \\ U(L) \end{Bmatrix} = \begin{Bmatrix} u(0) \\ u(1) \end{Bmatrix} = \begin{bmatrix} \mathbf{s}^T(0) \\ \mathbf{s}^T(1) \end{bmatrix} \mathbf{c} = \underbrace{\begin{bmatrix} 0 & 1 \\ \sinh(\mu) & \cosh(\mu) \end{bmatrix}}_{\mathcal{A}_{2 \times 2}} \mathbf{c} \quad (88)$$

The nodal force vector consists of the axial forces at the two ends of the beam. The displacement function $u(\xi)$ in Eq. (85) can be used to obtain them as

$$\mathbf{f} = \begin{Bmatrix} H_1 \\ H_2 \end{Bmatrix} = \begin{Bmatrix} -H(0) \\ H(L) \end{Bmatrix} = \frac{EA}{L} \begin{bmatrix} -\mathbf{s}^T(0) \\ \mathbf{s}^T(1) \end{bmatrix} \mathbf{c} = \frac{EA}{L} \underbrace{\begin{bmatrix} -\mu & 0 \\ \mu \cosh(\mu) & \mu \sinh(\mu) \end{bmatrix}}_{\mathcal{B}_{2 \times 2}} \mathbf{c} \quad (89)$$

In the above equation $(\bullet)'$ denotes the derivative with respect to ξ . Eliminating the constant vector \mathbf{c} from the previous two equations we obtain a direct relationship between the nodal force and displacement vectors as

$$\mathbf{f} = \frac{EA}{L} \underbrace{[\mathcal{B}_a \mathcal{A}_a^{-1}]}_{\mathcal{K}_{2 \times 2}} \delta \quad (90)$$

Using this expressions, the exact stiffness matrix for the axial case is given by Eq. (81) with two unique coefficients

$$a_1 = \mu \coth(\mu), \quad \text{and} \quad a_2 = \mu \operatorname{cosech}(\mu) \quad (91)$$

These expressions are similar to the expression of the axial dynamic stiffness matrix [22,23], except here hyperbolic functions are employed. The derivation proposed here does not use the shape functions and consequently avoids the determination of integrals

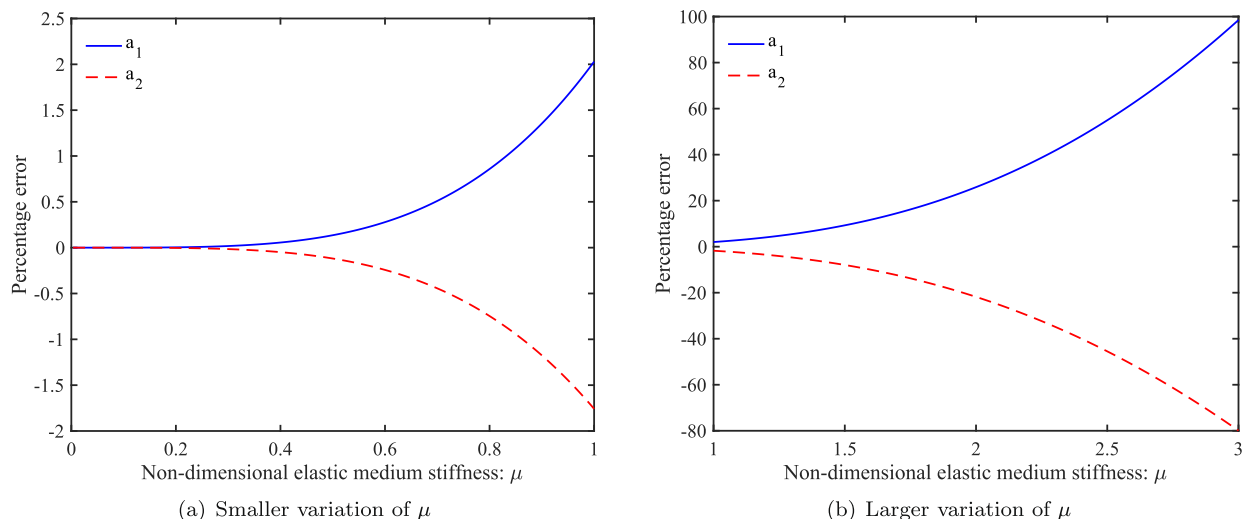


Fig. 9. Errors in the two unique axial stiffness coefficients obtained using the classical approach in comparison with the exact transcendental stiffness coefficients as functions of the non-dimensional elastic medium stiffness μ .

similar to what encountered in Eq. (79). It can be shown that the exact shape functions for the axial case is given by

$$\mathbf{N}(\xi) = \begin{bmatrix} -\coth(\mu) \sinh(\mu\xi) + \cosh(\mu\xi) \\ \operatorname{cosech}(\mu) \sinh(\mu\xi) \end{bmatrix} \quad (92)$$

Using these shape functions, the exact stiffness matrix can be alternatively obtained using Eq. (79).

There are two unique non-dimensional coefficients in the stiffness matrix in Eq. (90). They are functions of the elastic medium stiffness parameter μ only. Expanding them in a Taylor series about $\mu = 0$ we obtain

$$\begin{aligned} a_1 &= 1 + \frac{1}{3}\mu^2 - \frac{1}{45}\mu^4 + \frac{2}{945}\mu^6 - \frac{1}{4725}\mu^8 + O(\mu^{10}) \\ a_2 &= 1 - \frac{1}{6}\mu^2 + \frac{7}{360}\mu^4 - \frac{31}{15120}\mu^6 + \frac{127}{604800}\mu^8 + O(\mu^{10}) \end{aligned} \quad (93)$$

Considering only the first two terms in the above expansion, it can be confirmed that the stiffness matrix derived here reduces to the classical case in Eq. (82). Therefore, the higher-order terms quantify the extended effect of the elastic medium stiffness on the axial deflection of the beam. This analysis explicitly connects the transcendental stiffness coefficients with the classical stiffness coefficients. In Fig. 9, the error defined in Eq. (40) is shown for the two unique coefficients for different values of the non-dimensional elastic medium stiffness μ . Two different regimes have been selected, namely, $0 \leq \mu \leq 1$ and $1 \leq \mu \leq 3$. Note the significant difference in the values of the error for the two cases shown in Fig. 9(a) and Fig. 9(b). For values of $\mu > 1$, the difference between using the exact transcendental stiffness matrix and the classical stiffness matrix is significant. For this case, the proposed transcendental axial stiffness matrix should be used.

6.2. The combined stiffness matrix

The complete 6×6 stiffness matrix can be obtained by combining the bending and axial stiffness matrices from Eqs. (22) and (90). Considering the degrees-of-freedom described in Fig. 8, the bending and axial stiffness matrices should be combined into a single 6×6 stiffness matrix considering the respective indices. Using the notations in Eqs. (7) and (81), the general stiffness matrix can be expressed as

$$\mathbf{K}_g = \frac{EI}{L^3} \begin{bmatrix} \gamma a_1 & 0 & 0 & -\gamma a_2 & 0 & 0 \\ 0 & d_1 & d_2 L & 0 & -d_5 & d_6 L \\ 0 & d_2 L & d_3 L^2 & 0 & -d_6 L & d_4 L^2 \\ -\gamma a_2 & 0 & 0 & \gamma a_1 & 0 & 0 \\ 0 & -d_5 & d_6 L & 0 & d_1 & -d_2 L \\ 0 & -d_6 L & d_4 L^2 & 0 & -d_2 L & d_3 L^2 \end{bmatrix} \quad (94)$$

Here the non-dimensional factor γ is given by

$$\gamma = \frac{EA L^3}{L EI} = \frac{AL^2}{I} \quad (95)$$

For the rectangular and circular cross sections we can derive $\gamma = 12(L/t)^2$ and $\gamma = 4(L/r)^2$ respectively. Here t is the thickness of the rectangular beam and r is the radius of the circular beam. The expression and also the numerical value of γ can be obtained for other cross-sectional profiles using Eq. (95). Eq. (94) along with the definition of a_1, a_2 in Eq. (91) and $d_1 \dots d_6$ for the seven cases in Eqs. (36), (37), (44), (55), (63), (70) and (76) completely define the overall stiffness matrix of general beam columns in the most comprehensive, concise, clearer and universal manner. Due to the closed-form expressions and non-dimensional nature of these coefficients, they can be easily incorporated within a finite element framework in a convenient and efficient manner. The employment of the general stiffness matrix derived here will lead to superior

physical insights, higher accuracy and lower computational cost due to coarser discretisation owing to the exact nature of the underlying expressions.

The focus of this paper has been on the derivation of the stiffness matrices of general beam-columns embedded in elastic mediums. The engineering applications of the derived expressions will be in two broad directions. The first will be in the finite element analysis of large framework like structures where individual beams can be modelled as a single element without further discretisation. This will lead to computational efficiency. Both the response analysis and the eigenbuckling analysis can be carried out using the matrices derived here. The second direction will be in the analytical solution of bespoke mechanical problems involving beam-columns on elastic medium. Some examples include mechanics of carbon nanotubes embedded in substrates, analysis of railway tracks subjected to point and distributed loads, mechanics of pipelines embedded in the soil. As only a single 'element' is necessary, the present formulation will lead to closed-form expressions for the response and buckling load, providing physical insights and clarity on the parametric dependence.

7. Summary and conclusions

Stiffness matrices of general beam-columns embedded within an elastic medium are considered. Two approaches for deriving the stiffness matrix have been proposed. The first approach is based on the direct force-displacement relationship, while the second approach exploits shape functions within the scope of the finite element framework. Both approaches result in identical expressions when the exact displacement functions are used. The displacement function within the beam is obtained from the solution of the governing differential equation with suitable boundary conditions. The first approach is easier to implement in practice, and it does not involve any integration over the length of the beam. However, the second approach is more general as it can be applied to beams with non-uniform cross-section and take account of distributed body forces.

There is extensive literature available on the topic of the paper due to its classical nature. The novelty of this paper lies in (1) consistency and clarity in defining the element stiffness coefficients for different possible cases in a non-dimensional manner and (2) explicitly quantifying the accuracy of using the exact transcendental stiffness matrices over the classical stiffness matrix. It was shown that the 4×4 stiffness matrix for the bending deformation has in general six unique coefficients, while the 2×2 stiffness matrix for the axial deformation has two unique coefficients. The bending stiffness coefficients are expressed in terms of trigonometric and hyperbolic functions, whereas the axial stiffness coefficients are expressed in terms of hyperbolic functions only. Seven physically different cases are considered for the bending stiffness matrix, namely, (1) beam-columns with compressive axial force, (2) beam-columns with tensile axial force, (3) beams on elastic foundation and four additional parametric cases comprising beam-columns on an elastic foundation with compressive and tensile axial forces. Some of the key contributions of the paper are:

- A unified approach to the non-dimensional representation of the elements of the stiffness matrix and system parameters which is consistent across all the cases.
- The derivation of the transcendental shape functions based on the exact solution of the governing differential equation.
- Taylor-series expansions of the stiffness matrix coefficients and establishing direct correspondence with the equivalent classical expressions with lower-order terms.
- An explicit quantification of error using a universal metric.

The results obtained revealed that the use of a conventional stiffness matrix could lead to very large errors for beams embedded in an elastic medium. The relative error for the bending coefficients is larger compared to the axial coefficients. However, the impact of the axial force on the error in the bending stiffness coefficients is smaller than the foundation stiffness. The results derived here and the methodology developed to derive them can be extended to more advanced beam theories in future research.

Declaration of Competing Interest

The authors declare that they have no known competing financial interests or personal relationships that could have appeared to influence the work reported in this paper.

References

- [1] Carrera E, Giunta G. Refined beam theories based on a unified formulation. *Int J Appl Mech* 2010;2(01):117–43.
- [2] Thai H-T. A nonlocal beam theory for bending, buckling, and vibration of nanobeams. *Int J Eng Sci* 2012;52:56–64.
- [3] Reddy JN. Nonlocal theories for bending, buckling and vibration of beams. *Int J Eng Sci* 2007;45(2–8):288–307.
- [4] Zhang Y, Wang C, Challamel N. Bending, buckling, and vibration of micro/nanobeams by hybrid nonlocal beam model. *J Eng Mech* 2010;136(5):562–74.
- [5] Akgöz B, Civalek O. Strain gradient elasticity and modified couple stress models for buckling analysis of axially loaded micro-scaled beams. *Int J Eng Sci* 2011;49(11):1268–80.
- [6] Kong S, Zhou S, Nie Z, Wang K. Static and dynamic analysis of micro beams based on strain gradient elasticity theory. *Int J Eng Sci* 2009;47(4):487–98.
- [7] Dawe D. *Matrix and Finite Element Displacement Analysis of Structures*. Oxford, UK: Oxford University Press; 1984.
- [8] Paz M. *Structural Dynamics: Theory and Computation*. 2nd Edition. Reinhold: Van Nostrand; 1980.
- [9] Petyt M. *Introduction to Finite Element Vibration Analysis*. Cambridge, UK: Cambridge University Press; 1990.
- [10] Bathe K-J. *Finite Element Procedures*. Englewood Cliffs, New Jersey, USA: Prentice Hall Inc.; 1995.
- [11] Yankelevsky DZ, Eisenberger M. Analysis of a beam column on elastic foundation. *Comput Struct* 1986;23(3):351–6.
- [12] Bhattacharya S, Adhikari S, Alexander NA. A simplified method for unified buckling and dynamic analysis of pile-supported structures in seismically liquefiable soils. *Soil Dynam Earthquake Eng* 2009;29(8):1220–35.
- [13] Sirosh S, Ghali A, Razaqpur A. A general finite element for beams or beam-columns with or without an elastic foundation. *Int J Numer Methods Eng* 1989;28(5):1061–76.
- [14] Razaqpur A. Stiffness of beam-columns on elastic foundation with exact shape functions. *Comput Struct* 1986;24(5):813–9.
- [15] Karamanlidis D, Prakash V. Exact transfer and stiffness matrices for a beam/column resting on a two-parameter foundation. *Comput Methods Appl Mech Eng* 1989;72(1):77–89.
- [16] Reddy J. On locking-free shear deformable beam finite elements. *Comput Methods Appl Mech Eng* 1997;149(1–4):113–32.
- [17] Lignola GP, Spena FR, Prota A, Manfredi G. Exact stiffness–matrix of two nodes timoshenko beam on elastic medium. an analogy with eringen model of nonlocal euler–bernoulli nanobeams. *Comput Struct* 2017;182:556–72.
- [18] Hetenyi M. *Beams on Elastic Foundation: Theory with Applications in the Fields of Civil and Mechanical Engineering*. Ann Arbor, MI USA: University of Michigan Press; 1946.
- [19] Zienkiewicz OC, Taylor RL. *The Finite Element Method*. 4th Edition. London: McGraw-Hill; 1991.
- [20] Wittrick W, Williams F. A general algorithm for computing natural conditions of elastic structures. *Quart J Mech Appl Math* 1971;24(3):263–84.
- [21] Liu X. *On some eigenvalue problems for elastic instabilities in tension*, Ph.D. thesis, University of Glasgow; 2013.
- [22] Adhikari S, Murmu T, McCarthy M. Dynamic finite element analysis of axially vibrating nonlocal rods. *Finite Elem Anal Des* 2013;63(1):42–50.
- [23] Adhikari S, Murmu T, McCarthy M. Frequency domain analysis of nonlocal rods embedded in an elastic medium. *Physica E* 2014;59(5):33–40.